arXiv:0710.2002v1 [hep-ph] 10 Oct 2007

Transverse-momentum, threshold and joint resummations for slepton pair production at hadron colliders

Benjamin Fuks [a]

Laboratoire de Physique Subatomique et de Cosmologie, Université Joseph Fourier/CNRS-IN2P3,
53 Avenue des Martyrs, F-38026 Grenoble, France

Physikalisches Institut, Albert-Ludwigs-Universität Freiburg,
Hermann-Herder-Straße 3, D-79104 Freiburg i.Br., Germany

Abstract. We present precision calculations of the transverse-momentum spectrum and the invariant-mass distribution for slepton pair production at hadron colliders. We implement the transverse-momentum, threshold and joint resummation formalisms at the next-to-leading logarithmic accuracy and consistently match the obtained result with the pure perturbative result at the first order in the strong coupling constant, i.e. at $\mathcal{O}(\alpha_s)$. We give numerical predictions for selectron and stau pair production, and compare the various resummed cross sections with the perturbative result.

PACS. 12.60.Jv Supersymmetric models – 14.80.Ly Supersymmetric partners of known particles – 12.38.Cy Summation of perturbation theory

1 Introduction

One of the main goals of the experimental programme at present and future hadron colliders is to perform an extensive and conclusive search of the supersymmetric (SUSY) partners of the Standard Model (SM) particles predicted by the Minimal Supersymmetric Standard Model [1,2]. Scalar leptons are among the lightest supersymmetric particles in many SUSY-breaking scenarios, and often decay into the corresponding SM partner and the lightest stable SUSY particle, the distinctive signature at hadron colliders consisting thus in a highly energetic lepton pair and associated missing energy. Corresponding production cross sections have been extensively studied at leading order (LO) [3–7] and also at next-to-leading order (NLO) [8–10] of perturbative QCD.

The aim of this work is to perform an accurate calculation of the transverse-momentum (q_T) spectrum and to investigate the threshold-enhanced contributions, including soft-gluon resummation at the next-to-leading logarithmic (NLL) accuracy [10–12]. This allows for the reconstruction of the mass and the determination of the spin of the produced particles by means of the Cambridge (s)transverse mass variable [13,14] and for distinguishing thus the SUSY signal from the SM background, mainly due to WW and $t\bar{t}$ production [15,16].

When studying the transverse-momentum distribution of a produced slepton pair with an invariant mass M, it is convenient to separate the large- and small-q_T regions. For the large values of q_T the use of the fixed-order perturbation theory is fully justified, since the perturbative series is controlled by a small expansion parameter, $\alpha_s(M^2)$, but in the small-q_T region, where the bulk of the events will be produced, the coefficients of the perturbative expansion are enhanced by powers of large logarithmic terms, $\ln(M^2/q_T^2)$. As a consequence, results based on fixed-order calculations diverge as $q_T \to 0$, and the convergence of the perturbative series is spoiled. Furthermore, at the production threshold, when the initial partons have just enough energy to produce the slepton pair in the final state, the mismatch between virtual corrections and phase-space suppressed real-gluon emission leads also to the appearance of large logarithmic terms $[\ln(1-z)/(1-z)]_+$ where $z = M^2/s$, s being the partonic centre-of-mass energy. However, the convolution of the partonic cross section with the steeply falling parton distributions enhances the threshold contributions even if the hadronic threshold is far from being reached, i.e. $\tau = M^2/S \ll 1$, where S is the hadronic centre-of-mass energy, and in this intermediate z region, large corrections are expected for the Drell-Yan production of a rather light slepton pair at the CERN Large Hadron Collider (LHC). Accurate calculations of q_T-spectrum and invariant mass distribution must then include soft-gluon resummation in order to obtain reliable perturbative predictions and properly take these logarithmic terms into account.

The methods to perform all-order soft-gluon resummation at small q_T [17,18] and at large z [19–22] are well known. However, since the dynamical ori-

[a] *Email:* benjamin.fuks@physik.uni-freiburg.de

gin of the enhanced contributions is the same both in transverse-momentum and in threshold resummations, a joint resummation formalism has been developed in the last eight years, resumming the $\ln(M^2/q_T^2)$ and $[\ln(1-z)/(1-z)]_+$ terms simultaneously [12,23,24].

2 Resummation formalisms at the next-to-leading logarithmic level

In Mellin N-space, the hadronic cross section for the hard scattering process

$$h_a(p_a)\, h_b(p_b) \to \widetilde{l}\widetilde{l}^*(M, q_T) + X, \tag{1}$$

where a slepton pair with an invariant mass M and a transverse momentum q_T is produced, naturally factorizes

$$\frac{\mathrm{d}^2\sigma}{\mathrm{d}M^2\,\mathrm{d}q_T^2} = \sum_{a,b} \oint_{\mathcal{C}} \frac{\mathrm{d}N}{2\pi i}\, \tau^{-N}\, f_{a/h_a}(N+1)\, f_{b/h_b}(N+1) \times \frac{\mathrm{d}^2\hat{\sigma}_{ab}}{\mathrm{d}M^2\mathrm{d}q_T^2}(N). \tag{2}$$

$f_{a,b/h_{a,b}}$ are the N-moments of the universal distribution functions of partons a, b inside the hadrons $h_{a,b}$, $\hat{\sigma}_{ab}$ the relevant partonic cross section, and the contour $\mathcal{C}$ in the complex N-space will be specified in Sec. 3. The dependence on the unphysical renormalization and factorization scales μ_R and μ_F has been removed for brevity. In general, the corresponding partonic cross section can be written as

$$\mathrm{d}\sigma = \mathrm{d}\hat{\sigma}^{(\mathrm{res.})} + \mathrm{d}\hat{\sigma}^{(\mathrm{fin.})}, \tag{3}$$

where the resummed contribution is given by

$$\frac{\mathrm{d}\hat{\sigma}_{ab}^{(\mathrm{res.})}}{dM^2 dq_T^2}(N) = \int \frac{b}{2}\,\mathrm{d}b\, J_0(b\, q_T)\, \mathcal{W}_{ab}(N, b), \tag{4}$$

$$\frac{\mathrm{d}\hat{\sigma}_{ab}^{(\mathrm{res.})}}{\mathrm{d}M^2}(N) = \hat{\sigma}_{ab}^{(\mathrm{res})}(N), \tag{5}$$

for q_T spectrum and invariant-mass distribution, respectively. The impact-parameter b is the variable conjugate to q_T through a Fourier transformation, and $J_0(x)$ is the 0^{th}-order Bessel function. The perturbative functions $\mathcal{W}$ and $\hat{\sigma}$ embody the all-order dependence on the large logarithms and can be expressed in an exponential form,

$$\mathcal{W}_{ab}(N, b) = \mathcal{H}_{ab}(N) \exp\{\mathcal{G}(N, b)\}, \tag{6}$$

$$\hat{\sigma}_{ab}^{(\mathrm{res})}(N) = \sigma^{(LO)}\, \tilde{C}_{ab}(N)\, \exp\{\mathcal{G}(N)\}, \tag{7}$$

where $\sigma^{(LO)}$ is the LO cross section. The process-independent Sudakov form factor $\mathcal{G}$ allows to resum the soft-collinear radiation, while the process-dependent functions $\mathcal{H}$ and $\tilde{C}$ contain all the terms due to hard virtual corrections and collinear radiation. The general expressions of these functions can be found in Ref. [11] for transverse-momentum resummation, in Ref. [10] for threshold resummation and in Ref. [12] for joint resummation, so that an analysis at the NLL accuracy can be performed.

3 Inverse transform and matching

Once resummation has been achieved in N- and b-space (if relevant), inverse transforms have to be performed in order to get back to the physical spaces. Special attention has to be paid to the singularities in the resummed exponent, and the integration contours of the inverse transforms must therefore avoid hitting any of these poles. The b-integration is performed by deforming the integration contour with a diversion into the complex b-space [25], while the inverse Mellin transform is performed following a contour inspired by the Minimal Prescription [26] and the Principal Value Resummation [27].

In order to keep the full information contained in the fixed-order calculation and to avoid possible double-counting of the logarithmically enhanced contributions, a matching procedure of the NLL resummed cross section to the $\mathcal{O}(\alpha_s)$ result is performed through the formulae

$$\frac{\mathrm{d}^2\sigma}{\mathrm{d}M^2\,\mathrm{d}q_T^2} = \frac{\mathrm{d}^2\sigma^{(\mathrm{F.O.})}}{\mathrm{d}M^2\,\mathrm{d}q_T^2} + \oint_{C_N} \frac{\mathrm{d}N}{2\pi i}\, \tau^{-N} \int \frac{b\,\mathrm{d}b}{2} J_0(b\, q_T) \times \left[\frac{\mathrm{d}^2\sigma^{(\mathrm{res})}}{\mathrm{d}M^2\,\mathrm{d}q_T^2}(N, b; \alpha_s) - \frac{\mathrm{d}^2\sigma^{(\mathrm{exp})}}{\mathrm{d}M^2\,\mathrm{d}q_T^2}(N, b; \alpha_s)\right], \tag{8}$$

$$\frac{\mathrm{d}\sigma}{\mathrm{d}M^2}(\tau, M) = \frac{\mathrm{d}\sigma^{(\mathrm{F.O.})}}{\mathrm{d}M^2}(\tau, M) + \oint_{C_N} \frac{\mathrm{d}N}{2\pi i}\, \tau^{-N} \times \left[\frac{\mathrm{d}\sigma^{(\mathrm{res})}}{\mathrm{d}M^2}(N, M) - \frac{\mathrm{d}\sigma^{(\mathrm{exp})}}{\mathrm{d}M^2}(N, M)\right] \tag{9}$$

for q_T spectrum and invariant-mass distribution, respectively. $\mathrm{d}^2\sigma^{(\mathrm{F.O.})}$ is the fixed-order perturbative result, $\mathrm{d}^2\sigma^{(\mathrm{res})}$ is the resummed cross section and $\mathrm{d}^2\sigma^{(\mathrm{exp})}$ is the truncation of the resummed cross section to the same perturbative order as $\mathrm{d}^2\sigma^{(\mathrm{F.O.})}$.

4 Numerical results

We now present numerical results for slepton pair production at the LHC, with an hadronic centre-of-mass energy of $\sqrt{S} = 14$ TeV. For the LO (NLO and NLL) predictions, we use the LO 2001 [28] (NLO 2004 [29]) MRST sets of parton distribution functions and α_s is evaluated at two-loop accuracy. In the following, we choose the typical SUSY benchmark points SPS 1a, SPS 7 [30] and BFHK B [31] which gives, after the renormalization group evolution of the SUSY-breaking parameters performed by the `SPheno` [32] or `SuSpect` [33] programmes, light sleptons of 100-200 GeV and rather heavy squarks with masses in the 500-1000 GeV range.

In Fig. 1, we show the q_T-spectrum of a $\tilde{\tau}_1$ pair, for the benchmark point SPS 7, and we allow $\mu_F = \mu_R$ to vary between $M/2$ and $2M$ to estimate the perturbative uncertainty. We also integrate the equations of the previous sections with respect to M^2, taking as lower limit the energy threshold for $\tilde{\tau}_1\tilde{\tau}_1^*$ production and as upper limit the hadronic energy. The $\mathcal{O}(\alpha_s)$ result diverges, as expected, as $q_T \to 0$, while the effect of

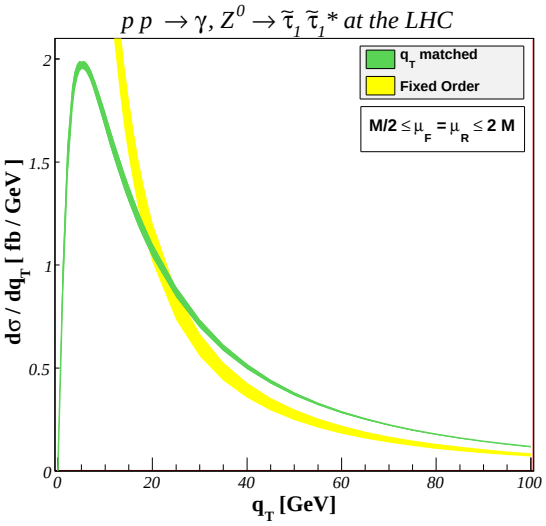


Fig. 1. Differential cross section for the process $pp \to \tilde{\tau}_1\tilde{\tau}_1^*$ at the LHC for the benchmark scenario SPS 7. NLL+LO matched result (with q_T resummation) and $\mathcal{O}(\alpha_s)$ result are shown.

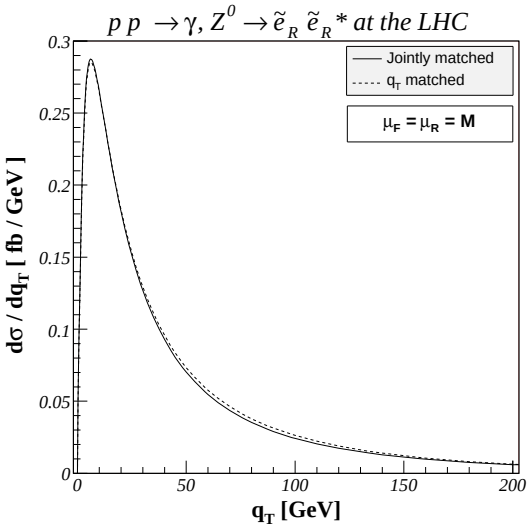


Fig. 2. Transverse-momentum distribution for selectron pair production at the LHC in the framework of joint (full) and q_T (dotted) resummations, for the benchmark point BFHK B.

resummation is clearly visible for small and intermediate values of q_T, the resummation-improved result being nearly 39% higher at $q_T = 50$ GeV than the pure fixed order result. Let us note that when integrated over q_T, the former leads to a total cross section of 66.8 fb in good agreement with the QCD-corrected total cross section at $\mathcal{O}(\alpha_s)$. The scale dependence is clearly improved with respect to the pure fixed-order calculations, being about 10% for the fixed order result, while it is always less than 5% for the matched curve.

In Fig. 2, we compare the jointly- and q_T-matched results for the production of a right-handed selectron pair, for the benchmark point BFHK B. The behaviour of the two curves is similar in the small-q_T region, while the jointly-resummed cross section is about 5%-10% lower than the q_T-resummed one for intermediate values of the transverse momentum q_T. This effect is thus clearly related to the threshold-enhanced contributions important in the large-M region, which are not present in q_T resummation.

For the scenario SPS 1a and $\tilde{\tau}_1$ pair production, we show in Fig. 3 the cross section correction factors

$$K^i = \frac{\mathrm{d}\sigma^i/\mathrm{d}M}{\mathrm{d}\sigma^{\mathrm{LO}}/\mathrm{d}M}, \tag{10}$$

where i labels the corrections induced by NLO QCD, additional NLO SUSY-QCD, resummation, the matched contributions as well as the fixed-order expansion of the resummation contribution as a function of the invariant mass M. In the left part of this plot, the matched result is less than 0.5% larger than the NLO (SUSY-)QCD result, since the slepton pair is produced with a relatively small invariant mass compared to the total available centre-of-mass energy, so that $z \ll 1$ and the resummation of $(1-z)$-logarithms is less important. Finite terms dominate the cross section and the resummed contribution is close to its fixed-order expansion. Only at large M the logarithms become important and lead to a 7% increase of the K-factor with resummation over the fixed-order result. In this region, the cross section is dominated by the large logarithms, and the resummed result approaches the total prediction, while the NLO QCD calculation approaches the expanded resummed result. In the intermediate-M region, we are still far from the hadronic threshold region and both resummed and fixed-order contributions are needed, a consistent matching being thus mandatory.

In Fig. 4, we eventually show the differences between threshold and joint resummations for $\tilde{e}_R$ pair production within the benchmark scenario BFHK B, which are only about one or two percents. These are due to the choices of the Sudakov form factor and of the $\mathcal{H}$-function, which correctly reproduce transverse-momentum resummation in the limit of $b \to \infty$, N being fixed, but which present some differences with pure threshold resummation in the limit $b \to 0$ and $N \to \infty$, as it was the case for joint resummation for Higgs and electroweak boson production [24,34]. However, this effect is under good control, since it is much smaller than the theoretical scale uncertainty of about 7%.

5 Conclusions

Within this work, soft-gluon resummation effects are now consistently included in predictions for various distributions for slepton pair production at hadron colliders, exploiting the q_T, threshold, and joint resummation formalisms. We found that the effects obtained from resumming the enhanced soft contributions are important, even far from the critical kinematical regions where the resummation procedure is fully justified. The numerical results show a considerable reduc-

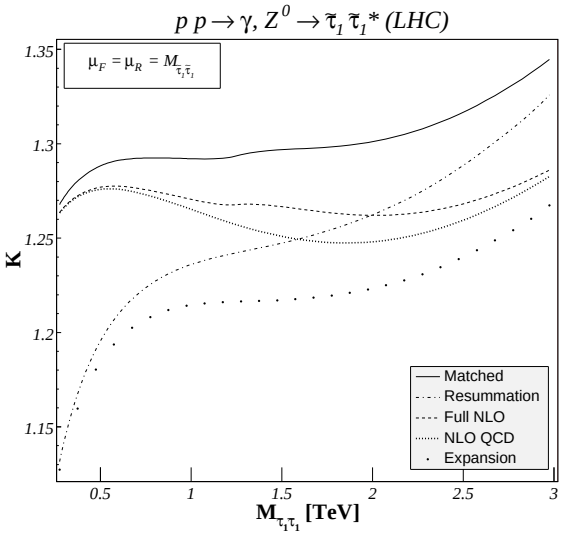


Fig. 3. K-factors as defined in Eq. (10) for $\tilde{\tau}_1$ pair production at the LHC for the benchmark point SPS 1a. We show the total NLL+NLO (threshold) matched result, the (threshold) resummed result at NLL, the fixed order NLO SUSY-QCD and QCD results, and the resummed result expanded up to NLO.

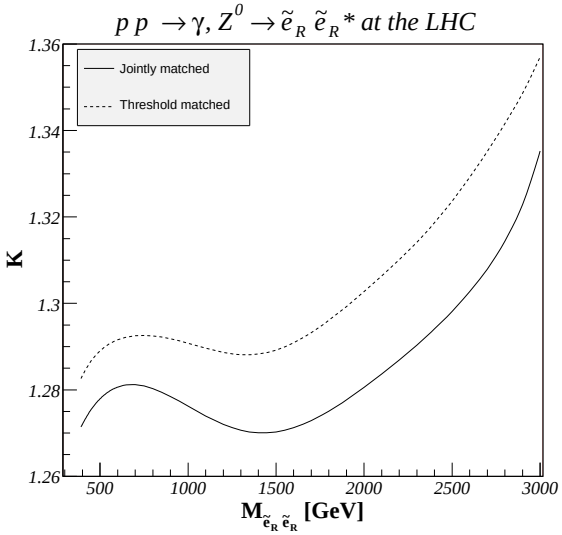


Fig. 4. K-factors as defined in Eq. (10) for $\tilde{e}_R$ pair production at the LHC for the benchmark point BFHK B. We show the total NLL+NLO jointly (full), and threshold (dashed) matched results.

tion of the scale uncertainty with respect to fixed order results, these features leading then to an increased stability of the perturbative results and thus to a possible improvement of the slepton pair search strategies at the LHC.

References

1. H. P. Nilles, Phys. Rept. **110** (1984) 1.
2. H. E. Haber and G. L. Kane, Phys. Rept. **117** (1985) 75.
3. S. Dawson, E. Eichten and C. Quigg, Phys. Rev. D **31** (1985) 1581.
4. P. Chiappetta, J. Soffer and P. Taxil, Phys. Lett. B **162** (1985) 192.
5. F. del Aguila and L. Ametller, Phys. Lett. B **261** (1991) 326.
6. H. Baer, C. H. Chen, F. Paige and X. Tata, Phys. Rev. D **49** (1994) 3283.
7. G. Bozzi, B. Fuks and M. Klasen, Phys. Lett. B **609** (2005) 339.
8. H. Baer, B. W. Harris and M. H. Reno, Phys. Rev. D **57** (1998) 5871.
9. W. Beenakker, M. Klasen, M. Krämer, T. Plehn, M. Spira and P. M. Zerwas, Phys. Rev. Lett. **83** (1999) 3780.
10. G. Bozzi, B. Fuks and M. Klasen, Nucl. Phys. B **777** (2007) 157.
11. G. Bozzi, B. Fuks and M. Klasen, Phys. Rev. D **74** (2006) 015001.
12. G. Bozzi, B. Fuks and M. Klasen, arXiv:0709.3057 [hep-ph].
13. C. G. Lester and D. J. Summers, Phys. Lett. B **463** (1999) 99.
14. A. J. Barr, JHEP **0602** (2006) 042.
15. E. Lytken, Czech. J. Phys. **54** (2004) A169.
16. Yu. M. Andreev, S. I. Bityukov and N. V. Krasnikov, Phys. Atom. Nucl. **68** (2005) 340.
17. S. Catani, D. de Florian and M. Grazzini, Nucl. Phys. B **596** (2001) 299.
18. G. Bozzi, S. Catani, D. de Florian and M. Grazzini, Nucl. Phys. B **737** (2006) 73.
19. G. Sterman, Nucl. Phys. B **281** (1987) 310.
20. S. Catani and L. Trentadue, Nucl. Phys. B **327** (1989) 323.
21. M. Kramer, E. Laenen and M. Spira, Nucl. Phys. B **511** (1998) 523.
22. S. Catani, D. de Florian and M. Grazzini, JHEP **0105** (2001) 025.
23. E. Laenen, G. Sterman and W. Vogelsang, Phys. Rev. D **63** (2001) 114018.
24. A. Kulesza, G. Sterman and W. Vogelsang, Phys. Rev. D **66** (2002) 014011.
25. E. Laenen, G. Sterman and W. Vogelsang, Phys. Rev. Lett. **84** (2000) 4296.
26. S. Catani, M. L. Mangano, P. Nason and L. Trentadue, Nucl. Phys. B **478** (1996) 273.
27. H. Contopanagos and G. Sterman, Nucl. Phys. B **419** (1994) 77.
28. A. D. Martin, R. G. Roberts, W. J. Stirling and R. S. Thorne, Phys. Lett. B **531** (2002) 216.
29. A. D. Martin, R. G. Roberts, W. J. Stirling and R. S. Thorne, Phys. Lett. B **604** (2004) 61.
30. B. C. Allanach *et al.*, Eur. Phys. J. C **25** (2002) 113.
31. G. Bozzi, B. Fuks, B. Herrmann and M. Klasen, arXiv:0704.1826 [hep-ph].
32. W. Porod, Comput. Phys. Commun. **153** (2003) 275.
33. A. Djouadi, J. L. Kneur and G. Moultaka, Comput. Phys. Commun. **176** (2007) 426.
34. A. Kulesza, G. Sterman and W. Vogelsang, Phys. Rev. D **69** (2004) 014012.